Phonon Critical Points Reflected in Superconducting Tunneling Characteristics

D. J. SCALAPINO
University of Pennsylvania, Philadelphia, Pennsylvania

AND

P. W. ANDERSON
Bell Telephone Laboratories, Murray Hill, New Jersey

(Received 11 September 1963)

Van Hove showed that there are mathematical singularities in the phonon distribution in frequency $g(\omega)$ associated with stationary points in $\omega(q)$ versus q; $dg/d\omega$ has at least two infinite discontinuities, and approaches $-\infty$ at the upper end of the spectrum. Additional weaker singularities have been discussed by Phillips. The current voltage characteristic of superconducting tunnel diodes exhibits structure related to the phonon spectrum; we investigate theoretically the nature of the mathematical singularities in the tunnel characteristic associated with the Van Hove and Phillips singularities, using the Eliashberg gap equation. Discontinuities and logarithmic singularities are predicted for the metal superconductor junction at $T=0$, and inverse square-root singularities as well in two-superconductor junctions. Analysis of Rowell's experimental curves for Pb and Sn in conjunction with neutron data on phonons in Pb provides definite evidence for the existence of such singularities and thus detailed confirmation of the theory.

I. INTRODUCTION

THE phonon density of states function $F(\omega)$ gives the number of phonon states (elastic frequencies) per unit frequency range. For a three-dimensional crystal, neglecting phonon damping, Van Hove[1] has shown that $dF/d\omega$ has at least two infinite discontinuities, and takes the value $-\infty$ at the upper end of the phonon spectrum. These singularities in $dF/d\omega$ are associated with stationary points in the $\omega(\mathbf{q})$ versus $\mathbf{q}$ frequency surfaces. Additional singularities of this same type can arise when different branches of the phonon frequency surfaces come in contact if there are no discontinuous components of $\nabla\omega(\mathbf{q})$ at the contact. These contact points can also produce weaker singularities (e.g., infinite discontinuities in $d^2F/d\omega^2$) when there are one or more discontinuous components of $\nabla\omega(\mathbf{q})$. The location of these so-called critical points, and the behavior of $F(\omega)$ near them, is an important characteristic of the phonon density of states. It has been made the basis of a method developed by Phillips[2] for calculating the main features of $F(\omega)$.

The energy gap parameter $\Delta(\omega)$ of a superconductor depends upon the phonon density of states, and is known to exhibit structure which is related to the location of the peaks in the phonon density of states.[3,4] This structure is reflected in the differential conductance versus voltage curves for a metal-superconductor tunnel junction.[5,6] The differential conductance is proportional to the effective tunneling density of states $N_T(\omega)$, which is given in terms of $\Delta(\omega)$ by[4]

$$N_T(\omega)=N(0)\ \mathrm{Re}\{\omega/[\omega^2-\Delta^2(\omega)]^{1/2}\}.$$

Here $N(0)$ is the density of Bloch states at the Fermi surface.

In addition to the structure in the conductance characteristic associated with the transverse and longitudinal peaks in the phonon density of states, Rowell, Anderson, and Thomas[7] have recently reported structure in the derivative of the conductance, which can be associated with the singularities in the derivatives of $F(\omega)$. These tunneling experiments therefore provide a direct method for the determination of critical points.

In this article, we analyze how the critical points of $F(\omega)$ are reflected as nonanalytic points in the I-V superconductor tunneling characteristic. We assume no phonon breadth, Δ a function of ω alone, and $T=0$; the former two are essential in all cases, $T=0$ only for the metal-superconductor case. The neglect of the phonon breadth due to the electron-phonon interaction is consistent with our integration of the gap equations, which neglects terms of order the square root of the electron to ion mass ratio. The anharmonic breadth, which is of this same order or somewhat larger, is also neglected. It is shown that the first derivative of the differential conductance, $d/dV(dI/dV)$, for a metal-superconductor (M-S) junction has a logarithmic singularity and a jump discontinuity at $V=\hbar\omega_c+\Delta_0$. Here ω_c is a critical point at which $dF/d\omega$ is infinite, Δ_0 is the energy gap, and V is the voltage across the junction measured in electron volts. For a two-superconductor (S-S) junction, this type of critical point in $F(\omega)$ produces an inverse square-root singularity in $(d/dV)(dI/dV)$ at $V=\hbar\omega_c+2\Delta_0$ if the superconductors are identical. Higher order critical points of the phonon spectrum produce singularities in the second and higher order

[1] L. Van Hove, Phys. Rev. **89**, 1189 (1953).
[2] J. C. Phillips, Phys. Rev. **104**, 1263 (1956).
[3] P. Morel and P. W. Anderson, Phys. Rev. **125**, 1263 (1963).
[4] J. R. Schrieffer, D. J. Scalapino, and J. W. Wilkins, Phys. Rev. Letters **10**, 336 (1963).
[5] I. Gaiever, H. R. Hart, Jr., and K. Megerle, Phys. Rev. **126**, 941 (1962).
[6] J. M. Rowell, A. G. Chynoweth, and J. C. Phillips, Phys. Rev. Letters **9**, 59 (1962).
[7] J. M. Rowell, P. W. Anderson, and D. E. Thomas, Phys. Rev. Letters **10**, 334 (1962).

derivatives of the M-S differential conductance. A certain class of these higher order critical points, associated with finite discontinuities in $dF/d\omega$, are shown to produce logarithmic singularities in $d/dV(dI/dV)$ for an S-S tunnel junction. Thus the derivative of the differential conductance of an S-S junction has singularities at all critical points where $F(\omega)$ has a discontinuous change in slope.

In Sec. II we review the relationship between the phonon density of states $F(\omega)$, the gap parameter $\Delta=\varphi/Z$, and the tunneling I-V characteristic. The set of coupled integral equations which determine the gap function φ and renormalization parameter Z in terms of F are given. In Sec. III these equations are analyzed for the case of an Einstein spectrum $F(\omega)\sim\delta(\omega-\omega_0)$. The real and imaginary parts of φ and Z are found to have characteristic square-root singularities at ω_0. Using these results, in Sec. IV we determine the nonanalytic behavior of the gap parameter and the effective tunneling density of states associated with critical points of $F(\omega)$. In Sec. V, the singularities of the first derivative of the differential conductance which reflect discontinuities in $dF/d\omega$ are obtained. In Sec. VI numerical comparisons with experimental results for Pb and Sn are given.

II. THE TUNNELING I-V CHARACTERISTIC AND THE PHONON DENSITY OF STATES

A tunnel junction consists of two metals which are separated by an oxide layer. The junction current is proportional to the transition rate for electrons to tunnel through the oxide layer. At low temperatures, and for applied voltages which are small compared to the Fermi energy, the important transfer processes involve electrons near the Fermi surfaces. The transition matrix element is essentially constant over the range of voltages considered, so that the I-V characteristic is determined by the effective tunneling density of states factors.

At $T=0$, the tunneling current from metal a to metal b is given by

$$I(V)=\text{const}\int_0^V d\omega N_T{}^b(\omega)N_T{}^a(\omega-V)\,,\qquad(1)$$

where $N_T{}^i$ is the effective tunneling density of states in metal i. For voltages small compared to the Fermi energy, the effective tunneling density of states for the normal state is given by $N(0)$, the density of Bloch states at the Fermi surface. For the superconducting state, Schrieffer, Wilkins, and one of the authors[8] have shown that

$$N_T(\omega)=N(0)\ \mathrm{Re}\{|\omega|/[\omega^2-\Delta^2(\omega)]^{1/2}\}\,.\qquad(2)$$

Here $\Delta(\omega)$ is the energy gap parameter, defined as the ratio of the gap function $\varphi(\omega)$ to the renormalization parameter $Z(\omega)$.

[8] D. J. S., see Ref. 4.

It is convenient to introduce the normalized phonon density of states $g(\omega)$

$$g(\omega)=F(\omega)\Big/\int d\omega F(\omega)\,.\qquad(3)$$

As is known,[9] the gap function $\varphi(\omega)$ and the renormalization parameter $Z(\omega)$ are related to $g(\omega)$ by the set of coupled integral equations

$$\varphi(\omega)=\int_{\Delta_0}^{\omega_c}d\omega'\ \mathrm{Re}\left\{\frac{\varphi'}{[(Z'\omega')^2-\varphi'^2]^{1/2}}\right\}\times\left\{\int d\omega_0\alpha^2(\omega_0)g(\omega_0)\times[D_{\omega_0}(\omega'+\omega)+D_{\omega_0}(\omega'-\omega)]-U\right\},\qquad(4)$$

$$(1-Z(\omega))\omega=\int_{\Delta_0}^{\omega_c}d\omega'\ \mathrm{Re}\left\{\frac{Z'\omega'}{[(Z'\omega')^2-\varphi'^2]^{1/2}}\right\}\times\int d\omega_0\alpha^2(\omega_0)g(\omega_0)[D_{\omega_0}(\omega'+\omega)-D_{\omega_0}(\omega'-\omega)],\qquad(5)$$

where $D_{\omega_0}(x)=(x+\omega_0-i0^+)^{-1}$, $\Delta_0=\varphi(\Delta_0)/Z(\Delta_0)$ is the gap parameter at the edge of the energy gap, and $\alpha(\omega)$ represents an effective electron-phonon coupling.[10] U is the Coulomb pseudopotential defined to include interactions between electrons outside a band of energies $|\omega|<\omega_c$ which is large compared to the Debye energy. Equations (4) and (5) are obtained by keeping only the lowest order electron-phonon vertex part, which neglects terms of order of the square root of the electron to ion mass ratio. In addition, the gap φ and renormalization parameter Z are assumed to be isotropic and homogeneous.

For a metal-superconductor junction, the conductance dI/dV is directly proportional to the effective tunneling density of states factor $N_T(V)$ of the superconductor. For a two-superconductor junction, the overlap of two factors involving $N_T(\omega)$ for a superconductor enters into the determination of the I-V characteristic. These density of states factors depend upon $\Delta=\varphi/Z$ and the functions φ and Z are determined by integrals over $F(\omega)$. Our program is to trace through the relationship between the I-V characteristic and the critical points at which $F(\omega)$ is nonanalytic. It turns out that the

[9] G. M. Eliashberg, Zh. Eksperim. i Teor. Fiz. 38, 966 (1960) [translation: Soviet Phys.—JETP 11, 696 (1960)].

[10] The effective electron-phonon coupling constant $\alpha(\omega_0)$ is defined by

$$\alpha^2(\omega_0)g(\omega_0)=[N(0)/8\pi p_F{}^2]\sum_\lambda\int qdqd\Omega_q|g_{q\lambda}|^2\delta(\omega_\lambda(q)-\omega_0)\,,$$

where $g_{\lambda q}$ is the dressed electron-phonon coupling constant, p_F is the Fermi momentum and $N(0)$ is the Bloch density of states at p_F. The index λ denotes the phonon polarization.

critical points in $F(\omega)$ are reflected as nonanalytic points in the I-V characteristics.

III. φ AND Z FOR AN EINSTEIN PHONON DISTRIBUTION

It is convenient to consider first the case of an Einstein phonon distribution $g(\omega)=\delta(\omega-\omega_0)$. The gap function φ and renormalization parameter Z given by Eqs. (4) and (5) depend upon ω_0 and will be labeled $\varphi(\omega,\omega_0)$, and $Z(\omega,\omega_0)$. The $\varphi(\omega)$ and $Z(\omega)$ functions for a general phonon distribution $g(\omega)$ will be obtained simply by integrating the Einstein results $\varphi(\omega,\omega_0)$, $Z(\omega,\omega_0)$ over the distribution $g(\omega_0)$. Since Eqs. (4) and (5) are nonlinear, this is not obviously the correct thing to do. The denominator $(Z^2\omega^2-\varphi^2)^{1/2}$ contains the solutions Z and φ of the integral equations, and since we find that Z and φ have singularities we should in principle discuss the interaction of these singularities with those in the numerator. This is the point at which we are able to enormously simplify the problem because of the fact that we are concerned only with the *most singular parts* of Z and φ.

Because this is the central part of our argument it may be well to indicate roughly how this works, which will also have the effect of indicating the framework of the rest of the paper. Let us think of our procedure as an iterative technique, starting from some approximate φ and Z which do not contain singularities and bringing in the singularities by stages. With a nonsingular φ and Z, the integrand has three singularities: The denominator $(Z'^2\omega'^2-\varphi'^2)^{1/2}$ has a square-root singularity at $\omega'=\Delta_0$, the function $g(\omega_0)$ is singular at the critical points $\omega_0=\omega_c$, and the D function at $\omega-\omega'=\omega_0$. (We note there is no reason to expect singularities in α.) All are integrable, so that the singularities of φ and Z will occur only where all coincide; i.e., at $\omega=\Delta_0+\omega_c$.

If the singularity in g were of δ-function form, the precise "Einstein model," the resulting singularity in φ would be of the form $(\omega-\Delta_0-\omega_c)^{-1/2}$, which is just as strong as the original singularity in the denominator. Then if we were to iterate (4) and (5) using the new φ containing this singularity we would have serious problems with the infinite propagation of singularities.

Fortunately, of course, the true singularities in g are at worst $1\frac{1}{2}$ orders weaker than $\delta(\omega_0-\omega_c)$; the most singular is of the form $(\omega_0-\omega_c)^{1/2}$. Then the iterated φ has singularities at worst of the form $(\omega-\Delta_0-\omega_c)\times\ln(\omega-\Delta_0-\omega_c)$. The effect of iterating such a weak singularity is very small; the functions $\varphi/(Z^2\omega^2-\varphi^2)^{1/2}$ and $Z/(Z^2\omega^2-\varphi^2)^{1/2}$ have no new singularities other than this one, and the coincidence of this singularity with those of g and D leads only to *still weaker singularities* at $\omega=\Delta_0+2\omega_c$ or, more generally, $\omega=\Delta_0+n\omega_{c_1}+m\omega_{c_2}+\cdots$.

Thus, in looking for the observable strongest singularities of φ and Z, it is unnecessary to take into account the nonlinear nature of (4) and (5). A convenient scheme which is equivalent to neglecting this is to do only the first iteration after interchanging the orders of integration in (4) and (5), integrating over ω_0 last. This is equivalent to integrating over a set of Einstein-model solutions of (4) and (5) in which the singular nature of φ and Z themselves has been ignored. This is the technique we follow, simply for the sake of mathematical convenience; but it should be emphasized that it is exact as to the form of the singularities and nearly so as to their magnitude.

Setting $D(x)=\mathrm{P}/(x+\omega_0)+i\pi\delta(x+\omega_0)$, we find that the imaginary parts of $\varphi(\omega,\omega_0)$ and $Z(\omega,\omega_0)$ for $\omega>0$ are given by

$$\operatorname{Im}\varphi(\omega,\omega_0)=\pi\alpha_0^2\operatorname{Re}\{\varphi(\omega-\omega_0,\omega_0)/[Z^2(\omega-\omega_0,\omega_0)(\omega-\omega_0)^2-\varphi^2(\omega-\omega_0,\omega_0)]^{1/2}\}\times\theta(\omega-\Delta_0-\omega_0);\quad(6)$$

$$\operatorname{Im}Z(\omega,\omega_0)=\pi\alpha_0^2\operatorname{Re}\{Z(\omega-\omega_0,\omega_0)(\omega-\omega_0)/[Z^2(\omega-\omega_0,\omega_0)(\omega-\omega_0)^2-\varphi^2(\omega-\omega_0,\omega_0)]^{1/2}\}\times\theta(\omega-\Delta_0-\omega_0).\quad(7)$$

Here $\theta(x)$ is the unit step function $\theta(x>0)=1$, and $\theta(x<0)=0$. Since $\Delta_0=\varphi(\Delta_0)/Z(\Delta_0)$, the imaginary parts of $\varphi(\omega,\omega_0)$ and $Z(\omega,\omega_0)$ have square-root singularities as ω approaches $\omega_0+\Delta_0$ from above. It follows that the functions $\varphi(\omega,\omega_0)$ and $Z(\omega,\omega_0)$ are analytic in the complex ω plane with cuts running from $\omega_0+\Delta_0$ to ∞ and $-\omega_0-\Delta_0$ to $-\infty$. The branch points at $\pm(\omega_0+\Delta_0)$ are square-root singularities. Therefore, the real parts of $\varphi(\omega,\omega_0)$ and $Z(\omega,\omega_0)$ will have square-root singularities as ω approaches $\omega_0+\Delta_0$ along the real axis from below or $-(\omega_0+\Delta_0)$ from above. φ and Z remain finite as ω approaches $\omega_0+\Delta_0$ along the real axis from above or $-(\omega_0+\Delta_0)$ from below.

The real parts of φ and Z are related to the Im parts of φ and Z by the usual dispersion relations which follow from the Cauchy identity, and are nothing more than the real parts of Eqs. (4) and (5).

$$\operatorname{Re}\varphi(\omega,\omega_0)=\int_{\Delta_0+\omega_0}^{\infty}\frac{d\omega'}{\pi}\frac{\operatorname{Im}\varphi(\omega',\omega_0)}{\omega'-\omega}+\int_{-\Delta_0-\omega_0}^{-\infty}\frac{d\omega'}{\pi}\frac{\operatorname{Im}\varphi(\omega',\omega_0)}{\omega'-\omega}+\varphi_c,\quad(8)$$

$$\operatorname{Re}Z(\omega,\omega_0)\omega=\int_{\Delta_0+\omega_0}^{\infty}\frac{d\omega'}{\pi}\frac{\operatorname{Im}Z(\omega',\omega_0)\omega'}{\omega'-\omega}+\int_{-\Delta_0-\omega_0}^{-\infty}\frac{d\omega'}{\pi}\frac{\operatorname{Im}Z(\omega',\omega_0)\omega'}{\omega'-\omega},\quad(9)$$

where φ_c is the constant Coulomb contribution to φ. For ω near the branch points $\pm(\omega_0+\Delta_0)$, the dominant contribution to the integrals in (8) and (9) is obtained for ω' near $\pm(\Delta_0+\omega_0)$. It is, therefore, an excellent approximation to replace $\varphi(\omega-\omega_0,\omega_0)/Z(\omega-\omega_0,\omega_0)$ by

Δ_0 in $\mathrm{Im}\varphi(\omega',\omega_0)$ and $\mathrm{Im}Z(\omega',\omega_0)$. The integrals can then be exactly evaluated, and we find, setting $\omega_c=\infty$,

$$\begin{aligned}\mathrm{Re}\varphi(\omega,\omega_0)-\varphi_c=&\frac{\Delta_0\alpha_0^2}{[(\omega_0+\omega)^2-\Delta_0^2]^{1/2}}\ln\left|\frac{\omega_0+\omega-\Delta_0+[(\omega_0+\omega)^2-\Delta_0^2]^{1/2}}{\omega_0+\omega-\Delta_0-[(\omega_0+\omega)^2-\Delta_0^2]^{1/2}}\right|\\&+\frac{2\Delta_0\alpha_0^2}{[\Delta_0^2-(\omega_0-\omega)^2]^{1/2}}\tan^{-1}(\Delta_0-\omega_0+\omega/\Delta_0+\omega_0-\omega)^{1/2},\quad|\omega-\omega_0|<\Delta_0\\=&\frac{\Delta_0\alpha_0^2}{[(\omega_0+\omega)^2-\Delta_0^2]^{1/2}}\ln\left|\frac{\omega_0+\omega-\Delta_0+[(\omega_0+\omega)^2-\Delta_0^2]^{1/2}}{\omega_0+\omega-\Delta_0-[(\omega_0+\omega)^2-\Delta_0^2]^{1/2}}\right|\\&+\frac{\Delta_0\alpha_0^2}{[(\omega_0-\omega)^2-\Delta_0^2]^{1/2}}\ln\left|\frac{\omega_0-\omega-\Delta_0+[(\omega_0-\omega)^2-\Delta_0^2]^{1/2}}{\omega_0-\omega-\Delta_0-[(\omega_0-\omega)^2-\Delta_0^2]^{1/2}}\right|,\quad|\omega-\omega_0|>\Delta_0;\end{aligned}\tag{10}$$

$$\begin{aligned}\mathrm{Re}(1-Z(\omega,\omega_0))\omega=&-\frac{(\omega_0+\omega)\alpha_0^2}{[(\omega_0+\omega)^2-\Delta_0^2]^{1/2}}\ln\left|\frac{\omega_0+\omega-\Delta_0+[(\omega_0+\omega)^2-\Delta_0^2]^{1/2}}{\omega_0+\omega-\Delta_0-[(\omega_0+\omega)^2-\Delta_0^2]^{1/2}}\right|\\&+\frac{2(\omega_0-\omega)\alpha_0^2}{[\Delta_0^2-(\omega_0-\omega)^2]^{1/2}}\tan^{-1}(\Delta_0-\omega_0+\omega/\Delta_0+\omega_0-\omega)^{1/2},\quad|\omega-\omega_0|<\Delta_0\\=&-\frac{(\omega_0+\omega)\alpha_0^2}{[(\omega_0+\omega)^2-\Delta_0^2]^{1/2}}\ln\left|\frac{\omega_0+\omega-\Delta_0+[(\omega_0+\omega)^2-\Delta_0^2]^{1/2}}{\omega_0+\omega-\Delta_0-[(\omega_0+\omega)^2-\Delta_0^2]^{1/2}}\right|\\&+\frac{(\omega_0-\omega)\alpha_0^2}{[(\omega_0-\omega)^2-\Delta_0^2]^{1/2}}\ln\left|\frac{\omega_0-\omega-\Delta_0+[(\omega_0-\omega)^2-\Delta_0^2]^{1/2}}{\omega_0-\omega-\Delta_0-[(\omega_0-\omega)^2-\Delta_0^2]^{1/2}}\right|,\quad|\omega-\omega_0|>\Delta_0.\end{aligned}\tag{11}$$

The real parts of $\varphi(\omega,\omega_0)$ and $Z(\omega,\omega_0)-1$ are plotted in Fig. 1. We note the following limiting results. In the low-frequency region

$$\begin{aligned}\Delta_0=&\mathrm{Re}[\varphi(\Delta_0,\omega_0)/Z(\Delta_0,\omega_0)]\\&\approx 2\omega_0\exp(-\omega_0/2\alpha_0^2)+\varphi_c+O(\Delta_0/\omega_0),\\&\mathrm{Re}Z(\Delta_0,\omega_0)\approx 1+2\alpha_0^2/\omega_0+O(\Delta_0/\omega_0).\end{aligned}\tag{12}$$

Here $O(\Delta_0/\omega_0)$ means that the corrections are of order Δ_0/ω_0. As the branch point $\Delta_0+\omega_0$ is approached from below, we find the expected square-root singularities in the real parts of φ and Z

$$\lim_{\omega\to\omega_0+\Delta_0-0_+}\mathrm{Re}\varphi(\omega,\omega_0)=\lim_{\omega\to\omega_0+\Delta_0-0_+}\mathrm{Re}\omega Z(\omega,\omega_0)\approx\frac{\pi\alpha_0^2(\Delta_0/2)^{1/2}}{(\omega_0+\Delta_0-\omega)^{1/2}}.\tag{13}$$

As ω approaches Δ_0 and ω_0 from above a finite limit is obtained:

$$\lim_{\omega\to\omega_0+\Delta_0+0_+}\mathrm{Re}\varphi(\omega,\omega_0)=-\lim_{\omega\to\omega_0+\Delta_0+0_+}\mathrm{Re}(1-Z(\omega,\omega_0)\omega=-\alpha_0^2.\tag{14}$$

In the high-frequency region $\omega/\omega_0\gg1$, the asymptotic forms are

$$\begin{aligned}\mathrm{Re}\varphi(\omega,\omega_0)&\approx-(2\Delta_0\alpha_0^2\omega_0/\omega^2)\ln\omega,\\\mathrm{Re}(1-Z(\omega,\omega_0))&\approx-2\alpha_0^2\omega_0/\omega^2.\end{aligned}\tag{15}$$

As previously noted, the weaker singularities associated with additional branch points at $(m\omega_0+\Delta_0)$ are neglected.

The singular behavior of the real and imaginary parts of φ and Z near the branch point $\omega_0+\Delta_0$ can be expressed in the simple form

$$\varphi_s(\omega,\omega_0)=\omega Z_s(\omega,\omega_0)=\pi\alpha_0^2(\Delta_0/2)^{1/2}/(\omega_0+\Delta_0-\omega)^{1/2}.\tag{16}$$

Here the subscript s denotes the "singular part of," and the $-i$ branch of the square root is taken for $\omega>\omega_0+\Delta_0$. Equation (16) is just a concise way of writing Eqs. (6), (7), and (13) when $\omega_0+\Delta_0\approx\omega$.

IV. THE BEHAVIOR OF $\Delta(\omega)$ ASSOCIATED WITH THE CRITICAL POINTS OF THE PHONON DENSITY OF STATES

In order to investigate the behavior of φ and Z associated with critical points of the phonon distribution, the Einstein model parameters $\varphi(\omega,\omega_0)$ and $Z(\omega,\omega_0)$ must be integrated over the normalized phonon density of states $g(\omega_0)$. The nonanalytic points, which we are interested in, arise from the overlap of the square-root singularities in $\varphi(\omega,\omega_0)$ and $Z(\omega,\omega_0)$ with the critical points of $g(\omega_0)$.

For critical points of $\omega(\mathbf{q})$ near which

$$\omega(\mathbf{q})=\omega_c+a\sum_\alpha\epsilon_\alpha(q_\alpha-q_{c_\alpha})^2,\tag{17}$$

Van Hove has shown that $g(\omega_0)$ contains a contribution

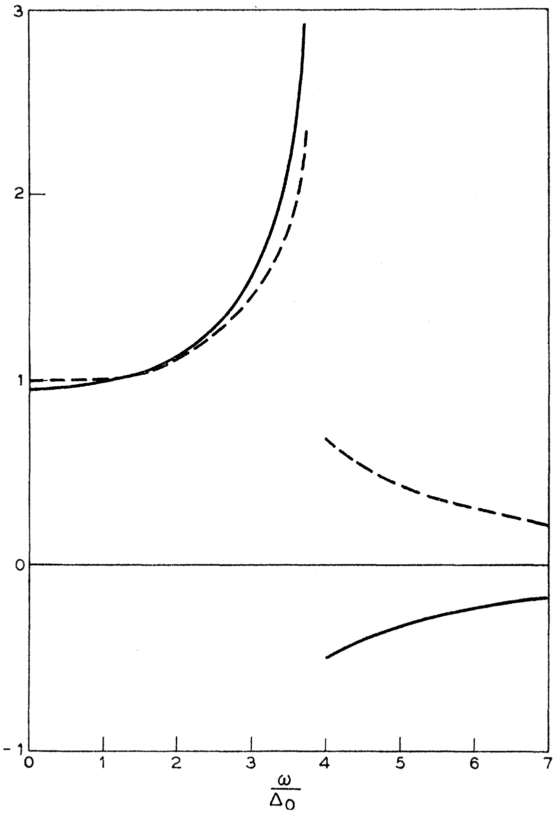

FIG. 1. Real parts of the φ and Z functions in the Einstein model. Solid: $[\mathrm{Re}\varphi(\omega,\omega_0)-\varphi_c]/[\mathrm{Re}\varphi_0-\varphi_c]$, where φ_0 is the value at the gap Δ_0. Dashed: $[\mathrm{Re}Z(\omega,\omega_0)-1]/\mathrm{Re}(Z_0-1)$. $\omega_0=3\Delta_0$.

proportional to $|\omega_c-\omega_0|^{1/2}$ as ω_0 approaches ω_c from one side of the critical point. For example, near a maximum in the $\omega(\mathbf{q})$ surface ($\epsilon_\alpha=-1$),

$$\begin{aligned} g(\omega_0)&=A+B(\omega_c-\omega_0)^{1/2}+O(\omega_c-\omega_0), & \omega_0<\omega_c \\ &=A+O(\omega_c-\omega_0), & \omega_0>\omega_c, \end{aligned} \tag{18}$$

where $B=2\pi v_0/3Za^{3/2}$. Here v_0 is the volume of the unit cell, Z is the number of atoms per unit cell, and a is the curvature coefficient defined by Eq. (17). Near a minimum $g(\omega_0)$ is given by interchanging ω_0 and ω_c in (18). At the saddle point S_1, characterized by $\epsilon_1=\epsilon_2=-\epsilon_3=+1$, the sign of the $(\omega_c-\omega_0)^{1/2}$ factor in (18) is negative. For the saddle point S_2, $\epsilon_1=\epsilon_2=-\epsilon_3=-1$, $g(\omega_0)$ is given by interchanging ω_0 and ω_c and changing the sign of the $(\omega_0-\omega_c)^{1/2}$ term.

Nonanalytic critical points of $\omega(\mathbf{q})$ produced by contacts between the various branches can also give rise to $|\omega_0-\omega_c|^{1/2}$ type singularities. In addition, weaker singularities at which $g(\omega_0)$ varies above or below ω_c as $|\omega_0-\omega_c|$, $|\omega_0-\omega_c|^{3/2}$, $(\omega_0-\omega_c)^2$ or $|\omega_0-\omega_c|^{3/2}\ln|\omega_0-\omega_c|$ can occur at branch contacts.[2] In the following discussion we will consider only the $|\omega_0-\omega_c|^{1/2}$ and $|\omega_0-\omega_c|$ variations since these are the only critical point behaviors which are reflected in d^2I/dV^2 as singularities where d^2I/dV^2 becomes infinite. We find that only the stronger variation, $|\omega_0-\omega_c|^{1/2}$, produces these singularities in d^2I/dV^2 for M-S junctions, while S-S junctions have such singularities associated with both the $|\omega_0-\omega_c|^{1/2}$ and the $|\omega_0-\omega_c|$ critical points of $g(\omega_0)$.

Integrating the singular parts of $\varphi(\omega,\omega_0)$ and $Z(\omega,\omega_0)$ given by (16) over a phonon distribution having an $|\omega_c-\omega_0|^{1/2}$ critical point at which $g(\omega_0)$ has the form (18), we find

$$\begin{aligned} &\int d\omega_0 g(\omega_0)\varphi_s(\omega,\omega_0) \\ &\quad\approx \pi C(\omega_c+\Delta_0-\omega)+iC(\omega-\omega_c-\Delta_0)\ln|\omega-\omega_c-\Delta_0|, \\ &\qquad\qquad \omega<\omega_c+\Delta_0 \\ &\quad\approx iC(\omega-\omega_c-\Delta_0)\ln|\omega-\omega_c-\Delta_0|, \quad \omega>\omega_c+\Delta_0 \end{aligned} \tag{19}$$

with a similar result for $\omega Z_s(\omega,\omega_0)$. Here $C=(\pi B/2)\times\alpha_0^2(\Delta_0/2)^{1/2}$. Then for values of ω near $\omega_c+\Delta_0$, the functions $\varphi(\omega)$ and $Z(\omega)$ have the following behavior

$$\begin{aligned} &\varphi(\omega)-\varphi^0(\omega) \\ &\quad=(Z(\omega)-Z^0(\omega))\omega \\ &\quad=\pi C(\omega_c+\Delta_0-\omega)+iC(\omega-\omega_c-\Delta_0)\ln|\omega-\omega_c-\Delta_0|, \\ &\qquad\qquad \omega<\omega_c+\Delta_0 \\ &\quad=iC(\omega-\omega_c-\Delta_0)\ln|\omega-\omega_c-\Delta_0|, \quad \omega>\omega_c+\Delta_0, \end{aligned} \tag{20}$$

where φ^0 and Z^0 are analytic in the neighborhood of $\omega_c+\Delta_0$. The results given above apply specifically to a critical point near which $g(\omega_0)$ is given by (18). As previously discussed, this corresponds to a maximum in the $\omega(\mathbf{q})$ surface. Near a minimum of $\omega(\mathbf{q})$, $g(\omega_0)$ is given by interchanging ω and ω_0 in (18). The resulting $\varphi(\omega)$ and $\omega Z(\omega)$ behavior near $\omega_c+\Delta_0$ for a minimum is

$$\begin{aligned} &\varphi(\omega)-\varphi^0(\omega) \\ &\quad=(Z(\omega)-Z^0(\omega))\omega \\ &\quad=C(\omega_c+\Delta_0-\omega)\ln(\omega_c+\Delta_0-\omega), \qquad \omega<\omega_c+\Delta_0 \\ &\quad=C(\omega_c+\Delta_0-\omega)\ln(\omega_c+\Delta_0-\omega)+i\pi C(\omega-\omega_c-\Delta_0), \\ &\qquad\qquad \omega>\omega_c+\Delta_0. \end{aligned} \tag{21}$$

For the saddle points S_1 and S_2 the variations of φ are given by Eqs. (20) and (21), respectively, with C replaced by $-C$.

Near a critical point of the type $|\omega_c-\omega_0|$, at which there is a finite change of slope, $g(\omega_0)$ has the form

$$\begin{aligned} g(\omega_0)&=C+S_1(\omega_0-\omega_c), & \omega_0<\omega_c \\ &=C+S_2(\omega_0-\omega_c), & \omega_0>\omega_c. \end{aligned} \tag{22}$$

In this case

$$\int d\omega_0 g(\omega_0)\varphi_s(\omega,\omega_0)=D(\omega_c+\Delta_0-\omega)^{3/2}, \tag{23}$$

where $D=(2\pi/3)\alpha_0^2\Delta_0(S_2-S_1)$ and the $+i$ branch of $(\omega_c+\Delta_0-\omega)^{3/2}$ is to be taken for $\omega>\omega_c+\Delta_0$. The nonanalytic part of $\omega Z(\omega)$ has the same form, and it follows that for ω near $\omega_c+\Delta_0$,

$$\varphi(\omega)-\varphi^0(\omega)=(Z(\omega)-Z^0(\omega))\omega$$
$$=[D/(\Delta_0/2)^{1/2}](\omega_c+\Delta_0-\omega)^{3/2}, \quad (24)$$

where φ^0 and Z^0 are analytic near $\omega_c+\Delta_0$.

When $\omega>|\Delta(\omega)|$, the effective tunneling density of states, Eq. (2), can be expanded in powers of $(\Delta(\omega)/\omega)^2$. Keeping only the lowest order correction, we have

$$N_T(\omega)/N(0)=1+(1/2\omega^2)\,\mathrm{Re}\Delta^2(\omega), \quad (25)$$

where $\Delta(\omega)=\varphi(\omega)/Z(\omega)$. In the region above the transverse peak in the phonon spectrum, this lowest order correction contains the major part of the deviation of $N_T(\omega)$ from $N(0)$. Writing

$$\frac{\Delta(\omega)}{\omega}=\frac{\varphi(\omega)}{\omega Z(\omega)}=\frac{\varphi^0(\omega)+\delta\varphi(\omega)}{\omega Z^0(\omega)+\delta(\omega Z(\omega))}$$

and expanding we find

$$\tfrac{1}{2}\,\mathrm{Re}\frac{\Delta^2(\omega)}{\omega^2}\approx\frac{1}{2\omega^2}\,\mathrm{Re}\Delta^{02}(\omega)+\frac{1}{\omega^2}\,\mathrm{Re}\left(\frac{\Delta^0(\omega)}{Z^0(\omega)}\delta\varphi(\omega)\right). \quad (26)$$

Here $\Delta^0(\omega)=\varphi^0(\omega)/Z^0(\omega)$, and $\delta\varphi=\varphi-\varphi^0$. Now, using the behavior of $\varphi-\varphi^0$ produced by an $|\omega_0-\omega_c|^{1/2}$ critical point, Eq. (20), the effective tunneling density of states for ω near $\omega_c+\Delta_0$ is given by

$$N_T(\omega)-N_T{}^0(\omega)=\frac{N(0)C}{\omega_t}\begin{cases}\beta\pi(\omega_c+\Delta_0-\omega)+\gamma(\omega_c+\Delta_0-\omega)\ln|\omega_c+\Delta_0-\omega|, & \omega<\omega_c+\Delta_0\\ \gamma(\omega_c+\Delta_0-\omega)\ln|\omega_c+\Delta_0-\omega|, & \omega>\omega_c+\Delta_0,\end{cases} \quad (27)$$

where

$$N_T{}^0(\omega)=N(0)(1+(1/2\omega^2)\,\mathrm{Re}\Delta^{02}(\omega)),$$
$$\Delta^0(\omega)=\varphi^0(\omega)/Z^0(\omega)$$

and

$$\beta=(\omega_t/\omega^2)\,\mathrm{Re}(\Delta^0/Z^0), \quad (28)$$
$$\gamma=(\omega_t/\omega^2)\,\mathrm{Im}(\Delta^0/Z^0). \quad (29)$$

Here ω_t is a frequency introduced to make β and γ dimensionless. For the numerical example of Pb, ω_t is taken as the center of the transverse phonon peak in $g(\omega_0)$. For the case of a minimum in the $\omega(\mathbf{q})$ surface, $N_T(\omega)-N_T{}^0(\omega)$ is given by interchanging ω with $\omega_c+\Delta_0$, and γ with $-\beta$ in (27). The results for a saddle point $S_1(S_2)$ are obtained by changing the sign of $N_T(\omega)-N_T{}^0(\omega)$ for the maximum (minimum).

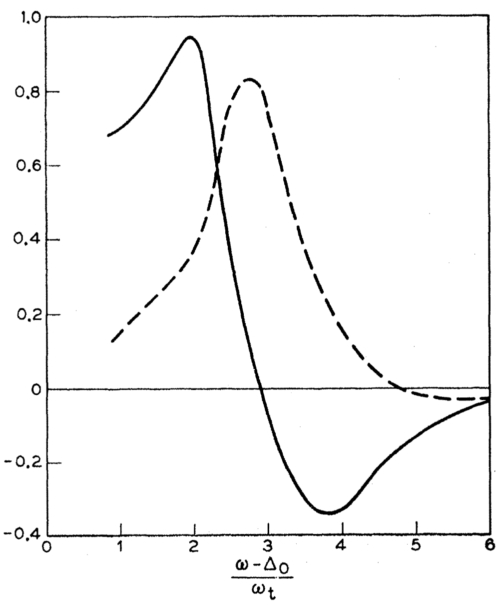

FIG. 2. β and γ, the singularity coefficients. β and γ as a function of frequency, as computed for Pb. β is solid, γ is dashed.

For an $|\omega_0-\omega_c|$ type critical point, the $\varphi-\varphi^0$ variation for ω near $\omega_c+\Delta_0$ is given by (24). Substituting this into (26) we find

$$N_T(\omega)-N_T{}^0(\omega)$$
$$=\frac{N(0)D}{\omega_t(\Delta_0/2)^{1/2}}\begin{cases}\beta(\omega_c+\Delta_0-\omega)^{3/2}, & \omega<\omega_c+\Delta_0\\ -\gamma(\omega-\omega_0-\Delta_0)^{3/2}, & \omega>\omega_c+\Delta_0.\end{cases} \quad (30)$$

The values of the parameters β and γ depend upon $\Delta^0=\varphi^0/Z^0$ and Z^0. The functions φ^0 and Z^0 are analytic in the neighborhood of $\omega_c+\Delta_0$. They represent the solution of the coupled integral Eqs. (4) and (5) for a phonon spectrum with the critical point at ω_c smoothed. Schrieffer, Wilkins, and one of the authors[11] have solved these equations for a model in which $g(\omega_0)$ is taken as a sum of two Lorentzians. The position and width of the Lorentzians were chosen to represent the Pb spectrum.[12] The results of this calculation provided an excellent fit of the over-all shape of the effective tunneling density of states and should provide a useful basis for determining β and γ for Pb. Using these results, the values of the parameters β and γ for Pb are plotted in Fig. 2.

We conclude this section with a brief discussion of the relationship between the variation of the density of states near a critical point and the phonon emission processes responsible for this variation. For the experimental comparison of Sec. VI it is useful to consider the case of the critical point at the end of the spectrum.

[11] D. J. S., see Ref. 4; J. R. Schrieffer, D. J. Scalapino, and J. W. Wilkins (to be published).

[12] The Lorentzians were centered at energies of 4.4×10^{-3} eV, 8.5×10^{-3} eV, and the half-widths were 0.75×10^{-3} eV and 0.5×10^{-3} eV, respectively. The lower of these two energies is the scale factor ω_t in Fig. 2.

TABLE I. The behavior of $d\sigma/dV$ associated with $|\omega_0-\omega_c|^{1/2}$ critical points.

$\lvert\omega_0-\omega_c\rvert^{1/2}$ Critical points	M-S $\lim_{V\to\Delta_0+\omega_c} \frac{d\sigma}{dV}$	M-S $\lim_{\epsilon\to 0}\left(\frac{d\sigma}{dV}\Big\rvert_{\Delta_0+\omega_c+\epsilon} - \frac{d\sigma}{dV}\Big\rvert_{\Delta_0+\omega_c-\epsilon}\right)$	S-S $\lim_{V\to 2\Delta_0+\omega_c-0^+} \frac{d\sigma}{dV}$	S-S $\lim_{V\to 2\Delta_0+\omega_c+0^+} \frac{d\sigma}{dV}$
Max	$-\frac{\gamma C}{\omega_t}\ln\lvert\omega_c+\Delta_0-V\rvert$	$\pi\beta C/\omega_t$	$(2\Delta_0)^{1/2}\frac{\pi\beta C}{\omega_t}\lvert V-\omega_c-2\Delta_0\rvert^{-1/2}$	$(2\Delta_0)^{1/2}\frac{\pi\gamma C}{\omega_t}\lvert V-\omega_c-2\Delta_0\rvert^{-1/2}$
Min	$-\frac{\beta C}{\omega_t}\ln\lvert\omega_c+\Delta_0-V\rvert$	$-\pi\gamma C/\omega_t$	$-(2\Delta_0)^{1/2}\frac{\pi\gamma C}{\omega_t}\lvert V-\omega_c-2\Delta_0\rvert^{-1/2}$	$-(2\Delta_0)^{1/2}\frac{\pi\beta C}{\omega_t}\lvert V-\omega_c-2\Delta_0\rvert^{-1/2}$
S_1	$\frac{\gamma C}{\omega_t}\ln\lvert\omega_c+\Delta_0-V\rvert$	$-\pi\beta C/\omega_t$	$-(2\Delta_0)^{1/2}\frac{\pi\beta C}{\omega_t}\lvert V-\omega_c-2\Delta_0\rvert^{-1/2}$	$-(2\Delta_0)^{1/2}\frac{\pi\gamma C}{\omega_t}\lvert V-\omega_c-2\Delta_0\rvert^{-1/2}$
S_2	$\frac{\beta C}{\omega_t}\ln\lvert\omega_c+\Delta_0-V\rvert$	$\pi\gamma C/\omega_t$	$(2\Delta_0)^{1/2}\frac{\pi\gamma C}{\omega_t}\lvert V-\omega_c-2\Delta_0\rvert^{-1/2}$	$(2\Delta_0)^{1/2}\frac{\pi\beta C}{\omega_t}\lvert V-\omega_c-2\Delta_0\rvert^{-1/2}$

Near the end point, the normalized density of states has the form (18) with $A=0$.

$$g(\omega_0)=B(\omega_c-\omega_0)^{1/2}, \quad \omega_0<\omega_c$$
$$=0 \qquad\qquad \omega_0>\omega_c.$$

Excited single-particle states decay by phonon emission. Their decay rate is proportional to the density of phonon and final single-particle states. The single-particle density of states is peaked with a square-root singularity at the gap edge Δ_0. As the energy of the single-particle state increases above $\omega_c+\Delta_0$ there is a sudden decrease in the phonon emission rate. This is because there are no longer any phonons capable of causing transitions in which the final single-particle energy approaches the gap edge. The convolution of the critical point variation at the end of the spectrum $(\omega_c-\omega_0)^{1/2}$, and the density of single-particle states near the edge of the gap $\omega/(\omega^2-\Delta^2)^{1/2}$ gives rise to a logarithmic singularity in the slope of the phonon emission rate at $\omega=\omega_c+\Delta_0$.

The imaginary part of the gap function $\varphi(\omega)$ is related to the decay rate of the single-particle state of energy ω. The logarithmic singularity in the slope of $\varphi(\omega)$ at $\omega=\omega_c+\Delta_0$, Eq. (20), is a direct reflection of the decrease in the phonon emission rate at this excitation energy. The variation of the effective tunneling density of states Eq. (26) is proportional to $-1/\omega^2\,\mathrm{Im}\Delta^0/Z^0 \times\mathrm{Im}(\varphi-\varphi_0)$ so that the logarithmic singularity in the slope of $\mathrm{Im}\varphi$ is reflected in the density of states, Eq. (27). It is this anomaly in the slope of $N_T(\omega)$ which produces the singularities in the derivative of the differential conductance which are discussed in the next section.

V. SINGULARITIES IN THE FIRST DERIVATIVE OF THE DIFFERENTIAL CONDUCTANCE

The differential conductance dI/dV for a metal-insulator-superconductor tunnel junction varies as $N_T(V)$. The first derivative of the differential conductance d^2I/dV^2 is therefore proportional to $dN_T(V)/dV$. It is convenient to normalize the differential conductance in the superconducting state by dividing it by what would be the differential conductance if the system were normal.

$$\sigma(V)=(dI/dV)_{\mathrm{super}}/(dI/dV)_{\mathrm{normal}}. \qquad (31)$$

This ratio approaches unity for $V\gg\Delta_0$. Then for an M-S junction

$$d\sigma(V)/dV=[1/N(0)]dN_T(V)/dV. \qquad (32)$$

For a critical point of the type $|\omega_0-\omega_c|^{1/2}$, we have from Eq. (27)

$$\lim_{V\to\Delta_0+\omega_c}\frac{d\sigma}{dV}\approx-\frac{\gamma C}{\omega_t}\ln|\omega_c+\Delta_0-V| \qquad (33)$$

and

$$\lim_{\epsilon\to 0}\left(\frac{d\sigma}{dV}\Big|_{\Delta_0+\omega_c+\epsilon}-\frac{d\sigma}{dV}\Big|_{\Delta_0+\omega_c-\epsilon}\right)=\frac{\pi\beta C}{\omega_t}. \qquad (34)$$

Therefore, if $dF/d\omega$ has an infinite square-root discontinuity at ω_c, the first derivative of the M-S differential conductance has a logarithmic singularity and a jump discontinuity at a voltage $V=\hbar\omega_c+\Delta_0$. Table I lists the variation of $d\sigma/dV$ at the minimum and saddle critical points. At all other critical points associated with weaker singularities in $F(\omega)$, d^2I/dV^2 for an M-S junction is continuous.

For a junction composed of two identical superconductors,[13] the tunneling current at an applied voltage V is

$$I(V)=\mathrm{const}\int_{\Delta_0}^{V-\Delta_0}d\omega N_T(\omega)N_T(\omega-V). \qquad (35)$$

[13] This simplification is clearly inessential; the second superconductor contributes only its gap edge singularity.

Using particle-hole symmetry, $N_T(\omega)=N_T(-\omega)$, we rewrite (35) in the form

$$I(V)=\text{const}2\int_0^{V/2-\Delta_0}d\omega N_T\left(\omega+\frac{V}{2}\right)N_T\left(\omega-\frac{V}{2}\right). \quad (36)$$

Setting $V=2\Delta_0+\omega_c+v$ and changing variables to $\omega'=\frac{1}{2}(\omega_c+v)-\omega$, the tunneling current is given by

$$I(2\Delta_0+\omega_0+v)$$
$$=\text{const}2\int_0^{(\omega_c+v)/2}d\omega' N_T(\omega'+\Delta_0)N_T(\omega_c+\Delta_0+v-\omega'). \quad (37)$$

For small v, the important contribution comes from the lower limit of the integration. In this region we have

$$N_T(\omega'+\Delta_0)/N(0)\approx(\Delta_0/2)^{1/2}(1/\omega')^{1/2}, \quad (38)$$

and for an $|\omega_0-\omega_c|^{1/2}$ critical point at which $g(\omega_0)$ is given by (18),

$$\frac{N_T(\omega_c+\Delta_0+v-\omega')}{N(0)}\approx\frac{C\gamma}{\omega_t}(\omega'-v)\ln|\omega'-v|$$
$$+\frac{\pi\beta C}{\omega_t}(\omega'-v)\theta(\omega'-v). \quad (39)$$

The integration in (37) can now be carried out, and we find for the derivative of the conductance ratio

$$\lim_{V\to2\Delta_0+\omega_c+0^+}\frac{d\sigma}{dV}\approx2\left(\frac{\Delta_0}{2}\right)^{1/2}\frac{\pi\gamma C}{\omega_t}\frac{1}{|V-\omega_c-2\Delta_0|^{1/2}}, \quad (40)$$

$$\lim_{V\to2\Delta_0+\omega_c-0^+}\frac{d\sigma}{dV}\approx2\left(\frac{\Delta_0}{2}\right)^{1/2}\frac{\pi\beta C}{\omega_t}\frac{1}{|V-\omega_c-2\Delta_0|^{1/2}}. \quad (41)$$

From (40) and (41) it follows that $d\sigma/dV$ for an S-S junction has a square-root singularity at $V=2\Delta_0+\hbar\omega_c$ if $dF/d\omega$ has a square-root singularity at ω_c. See Table I for the behavior of $d\sigma/dV$ for an S-S junction associated with minimum and saddle critical points.

For the case of an $|\omega_0-\omega_c|$ type critical point, at which $dF/d\omega$ has a finite discontinuity, it follows from (30) that

$$\frac{N_T(\omega_c+\Delta_0+v-\omega')}{N(0)}$$
$$\approx\frac{D}{\omega_t(\Delta_0/2)^{1/2}}\begin{cases}\beta(\omega'-v)^{3/2}, & \omega'>v\\ -\gamma(v-\omega')^{3/2}, & \omega'<v.\end{cases} \quad (42)$$

Carrying out the integration in (37) for this case,

$$\lim_{V\to2\Delta_0+\omega_c}\frac{d\sigma}{dV}\sim-\frac{\beta D}{\omega_t}\tfrac{3}{2}\ln|2\Delta_0+\omega_c-V| \quad (43)$$

and

$$\lim_{\epsilon\to0}\left(\left.\frac{d\sigma}{dV}\right|_{2\Delta_0+\omega_c+\epsilon}-\left.\frac{d\sigma}{dV}\right|_{2\Delta_0+\omega_c-\epsilon}\right)\approx-\frac{\gamma D}{\omega_t}\frac{3\pi}{2}. \quad (44)$$

Therefore, a critical point ω_c at which $F(\omega)$ has a finite change of slope produces a logarithmic singularity and a jump discontinuity in the derivative of the conductance for an S-S junction at a voltage $V=2\Delta_0+\hbar\omega_c$.

VI. COMPARISON WITH EXPERIMENT

Before attempting to identify the predicted singular behavior with features of the actual tunneling curves, it might be well to review the limitations of the assumptions made in the above theory. Certainly the most serious of these is implicit in the gap equations themselves [(4) and (5)]: the assumption that Δ and Z are functions of ω (energy) variables alone, not of momentum or, in the impure, thin film samples necessarily used in tunneling, of position within the sample. That the gap should not be seriously broadened by anisotropy can only be a result of the "dirty superconductor" effect, but even in the most carefully doped samples of Al, Masuda[14] found a gap distribution of about 2% (which in this case would be ~0.05 mV or ~0.5°K). Examination of the gap region of the current characteristic led Rowell[15] to believe that in the Pb samples on which our comparisons are based a broadening of nearer 5% or 0.15 mV at least is more realistic.

Phonon broadening from all sources has also been neglected. Probably impurity and surface scattering is most important, but in reasonably pure materials should not be serious.

A third problem is thermal broadening, especially in the metal-superconductor case in which a smearing effectively of several kT (~0.3–0.4 mV) may be expected. In principle, the superconductor-superconductor singularities should be sharp even at finite temperatures, but experimentally low temperatures seem to help in that case also.

In view of all these broadening sources, we do not expect to see the actual mathematical singularities predicted by the theory but broadened versions of them, only more or less identifiable as to position and shape and somewhat variable from sample to sample.

The most clear-cut case for comparison is that of Pb, where we have available a certain amount of neutron data on the phonon spectrum[16] as well as the best tunneling results for any metal.

[14] Y. Masuda, Phys. Rev. **126**, 1271 (1962).

[15] The data we use here are second derivative curves of tunnel current for Sn-SnO-Sn, Al-Al_2O_3-Pb_3, and Pb-PbO-Pb junctions, supplied us by J. M. Rowell, who has been of great assistance with their interpretation. Equivalent curves were reported in Ref. 7 and are to be published by J. M. Rowell. We are indebted very much to Dr. Rowell for permission to use his curves prior to publication.

[16] B. N. Brockhouse, T. Arase, G. Caglioti, K. R. Rao, and A. D. B. Woods, Phys. Rev. **128**, 1099 (1962).

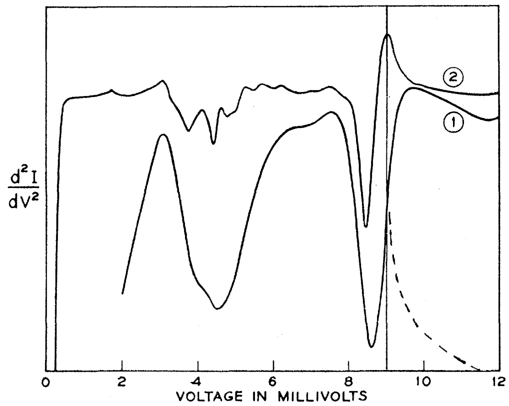

FIG. 3. Second derivative of tunnel current versus voltage for Pb-insulator-Al (1) and Pb-insulator-Pb (2) functions. The voltage scale is measured from Δ (1.4 mV) for (1) and from 2Δ for (2). The expected logarithmic singularity at 9 mV (in order of magnitude) is shown as a dashed line.

Figure 3 [15] is a tracing of some of the best examples of M-S (Al-Al_2O_3-Pb) and two-superconductor d^2I/dv^2 characteristics for Pb on a scale removing the shifts of the origin by Δ and 2Δ, respectively. Note the very much greater resolution in the two-superconductor case, caused, we suppose, both by the kT smearing in the M-S case and by the slightly higher order of the singularities.

The simplest, most interesting, and most complete test situation for our theory is the upper "longitudinal" region, around 9 mV on this plot. In this general region the Brockhouse data[16] locate a number of Van Hove singularities. The experimental data in the two-superconductor case at first glance looks like a single resonance-like structure, which may be associated with any or all of these singularities. The detailed theory permits us to disentangle some of this structure as well as to confirm the theory, an unexpected dividend.

The basic technique used is to slide a set of tracings of logarithmic or inverse-square-root curves over the data until a reasonable fit is achieved. Once the central point V_c of the singularity is known, one may check one's fit by an actual plot of the data against $\ln|V-V_c|$ or $|V-V_c|^{-1/2}$.

There are three essential criteria for a reasonable fit which seem, in several cases, to lead to a certain degree of uniqueness: (1) Those points which are neither too near the singularity (so that broadening effects do not mix in to some degree the other side of V_c) or too near other singularities should fit the appropriate curve; (2) the asymptotic value at reasonably large $|V-V_c|$ should not lie excessively far from the mean curve; and (3), and most important, the center of the singularity must fall in a reasonable region, neither in the smooth part of the curve nor too far from the obvious break associated with the singularity under consideration.

Figure 4 is an experimentally enlarged tracing of the region around 9 mV in the two-superconductor characteristic of Fig. 3. The resolution for this particular sample may not have been quite as good as that of Fig. 3 but the features are clearer.

The dashed curve on the right in Fig. 4 is a best $|V-V_c|^{-1/2}$ fit to this region of the data and the angle labeled (4) is the appropriate center position for the relevant singularity. It is important to note that any attempt to fit this region to a $\ln|V-V_c|$ singularity leads to a V_c in the smoothly rising part of the curve [violating (3) of our criteria] while an attempt to use a midpoint for this singularity which matches that of the left-hand region—i.e., assigning Fig. 4 to one large singularity—fails on the asymptotic condition. Thus we must assign this part of the curve to the last maximum—or the superposition of a number of nearby maxima—in the phonon spectrum. The arrows in Fig. 4 are singular points from the Brockhouse data, and we see that four maxima (for longitudinal waves in the [xxx], [$xx0$] and [$x00$] directions and for π waves in the square face) lie near the assigned position. While the tunnel current curves are reasonably reproducible to within say ± 0.05 mV, the singularity fit adds of the order of ± 0.1 mV uncertainty to this, so the accuracy is quite within the possible errors. We have checked the sign with Fig. 2, and estimate that the magnitude of the dotted curve is reasonable.

The rise on the left in Fig. 4 cannot, as we said, reasonably be assigned to the same singularity. A rough fit to a square root is shown; criterion (3) would move

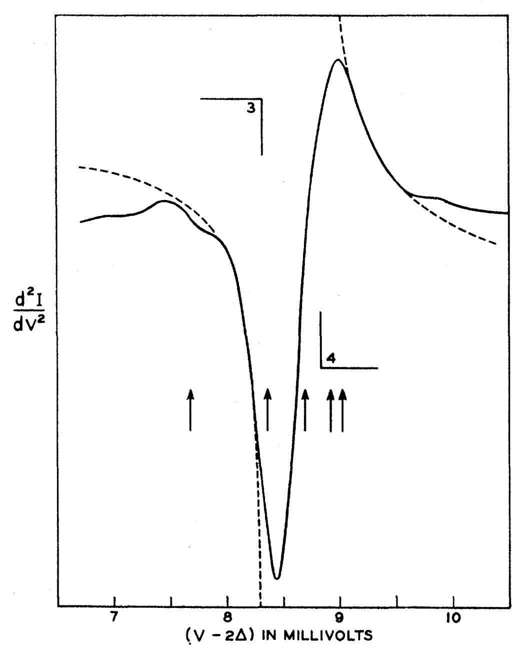

FIG. 4. Tracing of a large-scale experimental curve in the 9-mV region. Solid curve, tracing; dashed curves, $(V-V_c)^{-1/2}$ fits; right angles 3 and 4, origins of the singular functions; and the arrows are points of the Brockhouse data where $d\omega/dk=0$, likely Van Hove singularities.

TABLE II. Critical points of recognizable form observed in tunneling spectra.

Substance	Energy	Sign and type	Possible neutron assignment	Energy	Predicted sign
Pb	8.85±0.15 mV	$+\vert V-V_c\vert^{-1/2}$	L, xxx	9.05 mV	+
			L, $x00$	8.9	+
			L, $xx0$	8.7	+
			π	8.7	+
	8.35±0.15	$-\vert V-V_c\vert^{-1/2}$	T_2, $xx0$	8.35	+(?)
	7.75±?	?	T_2, $xx0$	7.65	−
	3.05±0.15	if $+\ln\vert V-V_c\vert$	none		
	3.25±0.15	if $+\vert V-V_c\vert^{-1/2}$			
Sn	3.5	if $+\vert V-V_c\vert^{-1/2}$			
	3.4	if $+\ln\vert V-V_c\vert$			
	17.7	$+\vert V-V_c\vert^{-1/2}$		max of spectrum	+

the center point "3" somewhat to the right. Note that the rise is interrupted near 7.6, where the Brockhouse data suggest another singularity. The sign of (3) suggests a minimum or S_1 point, which is not at first sight consistent with its being the Brockhouse point at 8.3 mV, which is a maximum in the T_2 mode along (110). Full phonon data would be necessary to establish this inconsistency; for the time being, we suggest that another singularity may be responsible.

These and the later Van Hove points suggested by our data analysis are summarized in Table II.

It is a little disturbing that the M-S characteristic (1) of Fig. 3 does not show any sign of the positive logarithmic singularity to be expected from Table I at the 8.9-mV point. The positive jump discontinuity is quite clear, as is the negative one associated with the $\sim$8.35 minimum; this verifies nicely the general conclusions of the theory. A rough estimate of the size of the logarithmic singularity is shown; it could, however, be smeared out by being a superposition of close maxima as we suggested. In addition, it is quite clear that kT smearing for the M-S characteristic is a really serious drawback. Perhaps the most we should have expected are the positive humps to either side of the negative well caused by the two jump discontinuties; even that seems a nicely detailed confirmation of Table I and its sign predictions.

The numerical estimate of the size of the logarithmic singularity is based on Table I, which shows that the coefficients of the discontinuity should be proportional to β where that of the logarithm is γ. Figure 2 gives γ as half of β at this point, so that, if we assign most of the singularity to the discontinuity β, we may guess the amplitude of the logarithm. Such calculations should also give us estimates of the magnitudes of the Van Hove singularities in the phonon spectrum, but absolute calibration of the second derivative curves is not easy.

In the lower region, around 4 mV, the structure is too complex to unravel separate singularities, except for the lowest one near 3 mV. Figure 5 is a large-scale plot of this region. A logarithmic curve centered at (1) is perhaps the best fit; the square root centered at (2) seems too far from the break in the curve. If this is a phonon (as the 1.8 mV structure is probably not) it does not lie on a symmetry direction; the nearest symmetric Van Hove's singularity is at 3.8 mV.

Another reason for suggesting that this is a "Phillips"

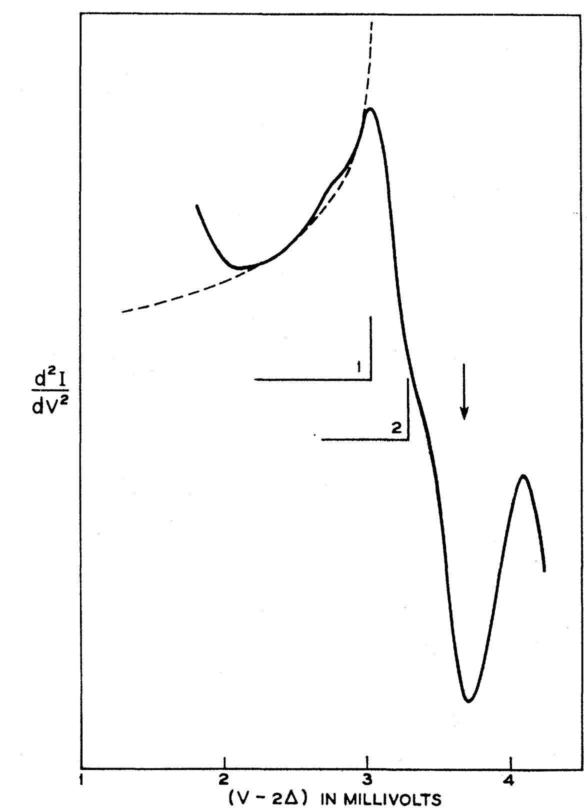

FIG. 5. Tracing of a large-scale experimental curve in the 4 mV region. Again the solid line is the tracing, the dashed line, the fit (a square-root function in this case), the right angles 1 and 2 are the possible origins. The lowest symmetric Van Hove point is denoted by an arrow.

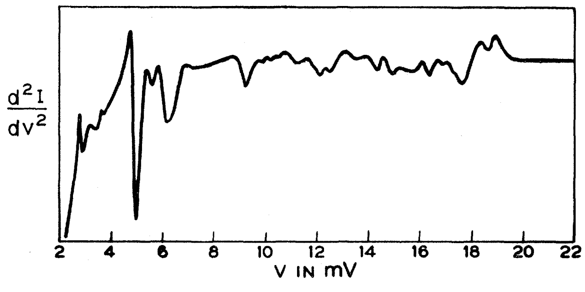

FIG. 6. Tracing of the full Sn insulator-Sn d^2I/dv^2 spectrum. Voltage scale reads from the origin.

singularity (a point where $g \sim |\omega - \omega_c|$) is that no recognizable structure in the M-S curve of Fig. 3 is associated with this point. True, the curve does go through a maximum but it is smooth and we notice that where the 9 mV singularity affected the curve for 0.2–0.5 mV to each side, there is no evidence of a precursor of this maximum; it seems merely to be the beginning of the 4–5 mV structure.

If, as this suggests, there is really such a point at 3 mV, it should be topologically a most interesting point: a band crossing in a general direction and lower than any minimum or saddle point. It will be interesting to see if more detailed phonon work bears out this rather unusual prediction.

Figure 6 shows a general tracing, with noise eliminated, of the two-superconductor Sn spectrum. It appears at first glance that the spectrum broadens and weakens very radically toward high energies, but it

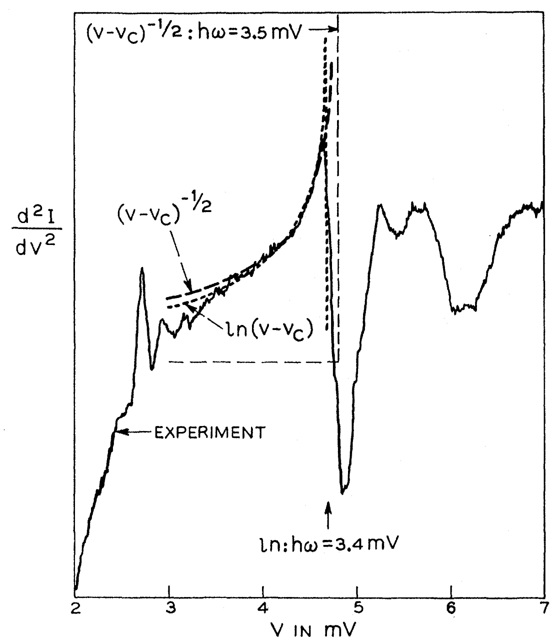

FIG. 7. A larger scale tracing of the 5 mV region. Two possible fits to the data are shown in dashed and dotted lines, a logarithmic and a square-root curve. Also shown are the resulting positions of the singularity.

must be realized that β and γ are proportional to ω^{-2} [see (28) and (29)], so that there is a weighting factor of 25 weakening the structure at 18 mV relative to that at 3.6; in other words, on an unbiased plot the 18-mV part would be off scale. It may well be that in the absence of noise the sharpness would also be comparable.

Nonetheless, the result is that reliable curve fitting is only possible at the low end. Figure 7 shows both types of fit to the lowest singularity. We have tried to trace out the "noise" (some of which is reproducible) as well as the general run of the data. We see that either fit will do: A logarithmic singularity at the break point or a square root, which then would have to account for the whole structure in this region.

The logarithm appears somewhat better, but not, probably, significantly so. An attempt to fit this with a hyperbola—just to see whether any real uniqueness could be claimed for this kind of fit—failed miserably.

FIG. 8. A fit to the maximum of the Sn spectrum. Solid line, tracing (magnitude of noise roughly indicated). Dashed line, $(V-V_c)^{-1/2}$ fit.

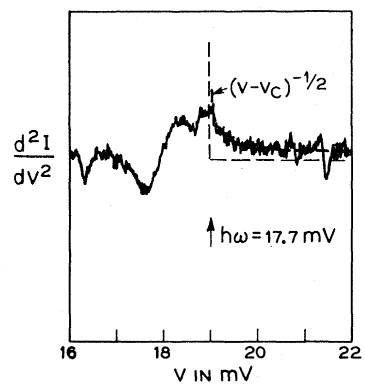

In Fig. 8 we show the topmost region of the Sn spectrum. In all of Figs. 6, 7, and 8 one must subtract out the gap $2\Delta = 1.3$ mV. A possible square-root fit to the maximum of the spectrum at $19 - 1.3 = 17.7$ mV is shown.[17]

VII. CONCLUSIONS

In this paper we have presented the theory of the effect of the Van Hove critical points in the phonon spectrum on the superconducting tunneling characteristic. As has been pointed out elsewhere,[4] there is reason to believe that in a certain limited sense the Eliashberg gap equations on which this theory is based are an exact solution of the problem, even in the strong coupling case, as in lead, where renormalization and damping effects are not small at all. The results one obtains for such things as the form of the singularities

[17] J. M. Rowell has called to our attention the calculation by M. J. P. Musgrave [Proc. Roy. Soc. (London) **A272**, 503 (1962)] of the phonon spectrum in white tin. The qualitative agreement with our results is good, especially in that Musgrave predicts remarkably low critical points for certain branches.

are completely different from those furnished by naive quasiparticle theory. Thus it is of real interest to work out these consequences and to subject them to as complete an experimental check as possible.

There is no clear inconsistency between theory and experiment, and in some cases it would be very hard to explain the data with other forms of singularity. We can claim a large number, then, of small but not conclusive checks on the theoretical predictions. In addition, the singularity analysis furnishes additional and quite precise information on the location and nature of the Van Hove singularities, which may be of value in analysis of phonon spectra of various metals.

ACKNOWLEDGMENTS

We wish to acknowledge the invaluable help at all stages of this work of J. R. Schrieffer and J. M. Rowell, as well as conversations on the interpretation of phonon spectra with J. C. Phillips.

PHYSICAL REVIEW VOLUME 133, NUMBER 4A 17 FEBRUARY 1964

Superconductivity of Solid Solutions of Ti and Zr with Co, Rh, and Ir

Ch. J. Raub
University of California, San Diego, La Jolla, California

AND

G. W. Hull, Jr.
Bell Telephone Laboratories, Murray Hill, New Jersey

(Received 14 October 1963)

A detailed investigation of superconductivity in α and β-Ti and Zr solid solutions with Co, Rh, and Ir showed that T_c rises with increasing valence electron concentration n. Small amounts of Co, Rh, and Ir dissolved in α-Ti, or α-Zr increase T_c by a factor of 2 to 4. In the bcc phase region of the β-Ti alloys T_c goes through a maximum of 4°K at 90 at.% Ti, which is explained by Matthias' rule.

I. INTRODUCTION

It has been shown by Matthias and co-workers that the transition temperature of α-Ti is increased more by the addition of Fe than by the addition of an equal amount of Ru.[1] Since both elements have the same number of valence electrons, the phenomenon was explained by a magnetic interaction. It therefore seemed interesting to investigate the effect of the Co-group elements, Co, Rh, and Ir, on the transition temperatures of Ti and Zr.

Previous superconducting studies include the Ti and the Zr solid solutions with Co and Rh. Since the superconductivity of[1] Ti-Co solid solutions had been investigated thoroughly, only a few alloys in the Ti hcp and bcc regions were prepared in the current study. The previous results are confirmed. The transition temperature of a Zr alloy containing 10 at.% Co has been reported as 3.9°K.[2] Recently, the superconductivity of Ti-Rh and Zr-Rh solid solutions in the α and β regions has been investigated.[3,4]

Since there is no information in the literature about the superconducting properties of Ti and of Zr solid solutions with Ir and only limited data for Zr-Co solid solutions, we concentrated our investigations on these systems. A few additional solid solutions in the Ti-Rh system were also studied.

II. EXPERIMENTS

Of greatest importance in working with Ti and Zr alloys is the purity. Not only metallic impurities, but also oxygen and nitrogen contaminations, change the behavior of these alloys in various ways, as shown by Raub and Röschl[5] for the Ti-Ru and Zr-Ru alloys. They may influence T_c directly or change the thermodynamic stabilities of the different modifications. Most dilute Ti and Zr alloys show a martensitic transformation of the bcc β modification into a hcp α' form, which has the same crystal structure and lattice constant as the low-temperature α modification, but different concentration. During appropriate heat treatment α' transforms into the stable α modification. The yields of the β, α, α' phases depend not only on the concentration or rate of cooling, but also on the purity of the components, e.g., it is well known that oxygen and nitrogen contaminations tend to stabilize the α-Zr modification. In general, one can predict that if the eutectoid is much lower than the $\beta \rightarrow \alpha$ transformation temperature of the pure

[1] B. T. Matthias, V. B. Compton, H. Suhl, and E. Corenzwit, Phys. Rev. **115**, 1597 (1959).
[2] B. T. Matthias and E. Corenzwit, Phys. Rev. **100**, 626 (1955).
[3] Ch. J. Raub and C. A. Andersen, Z. Physik **175**, 105 (1963).
[4] W. Buckel, G. Dummer, and W. Gey, Z. Angew, Physik **14**, 703 (1962); Phys. Kondens Materie **1**, 66 (1963).
[5] E. Raub and E. Röschl, Z. Metallk. **54**, 455 (1963).